

Supporting Information for the Article

Intermetallic Species in the Negishi Coupling and Their Involvement in Inhibition Pathways

Mikhail V. Polynski†‡ and Evgeny A. Pidko*†⊥*

† TheoMAT group, ITMO University, Lomonosova 9, St. Petersburg, 191002, Russia

‡ Zelinsky Institute of Organic Chemistry, Russian Academy of Sciences, Leninsky prospekt 47,
Moscow, 119991, Russia

⊥ Current address: Inorganic Systems Engineering group, Department of Chemical Engineering,
Delft University of Technology, Van der Maasweg 9, 2629 HZ Delft, The Netherlands

* polynskimikhail@gmail.com (M.V.P.); e.a.pidko@tudelft.nl (E.A.P.)

Table of Contents

1. COMPUTATIONAL DETAILS.....	S2
2. ENERGETICS OF THE ELEMENTARY STEPS	S7
3. QTAIM ANALYSIS RESULTS	S34
4. RELAXED SURFACE SCAN RESULTS.....	S35
5. TOTAL AND RELATIVE ENERGIES OF LI ZINCATE SPECIES.....	S37
6. THERMODYNAMICS OF THE FORMATION OF ZN-M(II)-INTERMETALLIC SPECIES IN NHC-LIGAND CATALYTIC SYSTEMS	S38
7. REFERENCES.....	S40

1. Computational details

The ORCA program (ver. 4.0.1)¹ was used to perform restricted Kohn-Sham DFT computations. The Gibbs free energies were computed at two levels of theory. First, the B97-3c method² was used which is the combination of the re-parameterized B97 GGA functional³ with a set of empirical corrections. In B97-3c calculations, the Kohn-Sham wavefunction is approximated with the specifically optimized def2-mTZVP basis set. The B97-3c method is implemented with the resolution-of-identity (RI) approximation⁴⁻¹⁰ (def2-mTZVP/J is used as an auxiliary basis set).

Second, we used the meta-GGA TPSS functional¹¹ with the empirical corrections for dispersion interactions (D3(BJ)-correction including three-body terms)^{12,13} and the basis set superposition error (gCP-correction).¹⁴ The def2-SVP basis set¹⁵ and the Stuttgart-Dresden “def2-SD” effective core potentials for Pd¹⁶ and I¹⁷ were used. The RI approximation was applied as well with Def2/J as an auxiliary basis set.¹⁸ The restricted Kohn-Sham approach with tight convergence criteria (TightSCF) was used for calculations *in vacuo*. A dense integration grid (GRID6) with the multigrid feature turned off (NOFINALGRID) was used to calculate energies in computations at the B97-3c and RI-TPSS-D3(BJ)/def2-SVP-gCP levels of theory (we denote the latter as TPSS-D3/DZP).

Frequency calculations were performed using the finite difference method (NUMFREQ procedure) to check whether the optimized geometries are true minima and to compute the free Gibbs energies. The vibrational entropy terms were computed within the QRRHO formalism.¹⁹ Accordingly, the ΔG_{QRRHO}^A term in Equations (1) and (2) of the main text includes:

$$\Delta G_{QRRHO}^A = E_{ZPE} + E_{vib} + E_{rot} + E_{trans} + RT + S_{vib} + S_{rot} + S_{trans},$$

Where E_{ZPE} is zero-point energy, E_{vib} is thermal correction due to population of excited vibrational states, E_{rot} is thermal rotational energy, E_{trans} is thermal translational energy, RT is universal gas

constant multiplied by system temperature (298.15 K), S_{vib} is vibrational entropy in QRRHO approximation, S_{rot} is rotational entropy, S_{trans} is translational entropy (all terms computed for molecules *in vacuo*).

Solvent coordination was accounted via explicit inclusion of THF molecules in the model systems when solvent to intermediate binding was observed in test optimization runs. The C-PCM model was used to account for bulk solvent effects (default parameters for the THF solvent).²⁰ The C-PCM calculations were performed as the separate geometry optimization runs with the starting structures, previously optimized *in vacuo*, at the same level of theory (B97-3c or TPSS-D3/DZP). In the C-PCM calculations, the same calculation parameters (see above), except for the convergence criteria in the Kohn-Sham self-consistent field procedure (KS-SCF), were used. Because of poor numerical stability of the KS-SCF procedure in the performed C-PCM calculations, the “NormalSCF” criteria were selected with the “VerySlowConv” parameter set for the procedure.

Relaxed surface scans were performed at the B97-3c or TPSS-D3/DZP levels of theory with the bulk solvent effects accounted for with C-PCM; the same converger parameters (“NormalSCF” and “VerySlowConv”) were set.

We performed quasi-relativistic all-electron computations *in vacuo* with the TPSS functional and the ZORA-def2-TZVP basis set (see ORCA manual and Ref. 15) for QTAIM analysis. The quasi-relativistic computations were performed with the point nucleus model and the ZORA method²¹ as implemented with the model potential (the nuclear attraction, Coulomb, and VWN-5 local correlation terms included).²² The one-center approximation (“OneCenter true”) was used. In all-electron computations, the restricted Kohn-Sham procedure with the tight convergence criteria (TightSCF) was chosen. In this case, we used an unpruned dense integration grid (GRID7)

with the multigrid feature turned off (NOFINALGRID) and the number of radial points increased from the default value (IntAcc parameter equal to 10.0). The “old-ZORA-TZVP” basis sets were used for Pd and I. A Coulomb fitting basis set from the standard library (SARC/J) was used in the quasi-relativistic computations since the RI-approximation was used in this case as well.^{18,23}

AIMAll program (version 17.01.25) was used for the QTAIM analysis. The “Complex” mechanism for determination of critical point connectivity was used.²⁴ The Proaim algorithm²⁵ with a “Very Fine IAS mesh” and a basin quadrature of a “Very High” accuracy was chosen for basin integration in most cases, except those (explicitly stated) when an automatic choice of an integration algorithm (AIMAll default) with “Very Fine IAS mesh” was used. This was necessary as in some model systems the integration with the aforementioned parameters did not give consistent results. In the latter case, all atoms were integrated using the Proaim or Promega algorithms and a basin quadrature of adaptive accuracy. Atomic source contributions were calculated in all cases.

Li zincates were modeled as contact ionic pairs at the RI-TPSS-D3(BJ)/ma-def2-SVP level. All parameters were kept the same as in TPSS-D3/DZP calculations (see above), except the following. As mentioned, the diffuse ma-def2-SVP basis set was used to account for non-valent ionic interactions;²⁶ the empirical gCP corrections were not used in this case. Since we applied RI approximation, and no auxiliary basis set for the diffuse ma-def2-SVP basis set is available in ORCA, we used the “OldAutoAux” procedure for the generation of the auxiliary basis set. Molecular structure of ionic pairs may differ significantly in vacuum and in solution. Therefore, we abstained from considering the geometries in vacuum and performed geometry optimizations, only applying C-PCM. Computation of thermochemical corrections (the ΔG_{QRRHO}^A term) implies calculations of vibrational frequencies; the validity of vibrational frequency calculations with the

application of continuum solvation models (here, C-PCM) is a matter of an ongoing debate.²⁷⁻²⁹ Because of this, we abstained from the inclusion of the ΔG_{QRRHO}^A term in estimations of thermodynamic effect of reactions involving the ionic pairs. In such a way, energies of the ionic pair species E^A were approximated as the following sum:

$$E^A = E_{sol}^A + \Delta G_{solv,non-var}^A \quad (1),$$

Where E_{sol}^A is the total energy of ionic pair species A in THF (includes total electron energy, empirical D3(BJ) correction, and variational C-PCM part), and $\Delta G_{solv,non-var}^A$ includes the corresponding non-variational C-PCM terms.

As long as the diffuse basis set ma-def2-SVP was used in conjunction with C-PCM, special tuning of the SCF procedure was needed to achieve the numeric stability of the procedure; Fock matrices were recalculated on each KS-SCF iteration (“DirectResetFreq” equal to 1), and 15 Fock matrices were stored in memory (“DIISMaxEq” equal to 15).

We performed vibrational frequency analysis (NUMFREQ) to ensure that the optimized geometries of the ionic pairs are energy minima. Imaginary frequencies were found in only one case. In the optimized $\text{Li}_2[\text{ZnBr}_4]$, two vibrations of both Li atoms had imaginary frequencies. All data on these vibrations were included in the supporting ZIP archive with the corresponding molecular structures in XYZ format. Apparently, vibrations of Li atoms cause a significant redistribution of surface charges in C-PCM, which, in turn, can lead to numerical discontinuities (known issue, see Ref. 30). Note, that upon the change of the so-called epsilon function in C-PCM to a non-default value (“fepstype cosmo”), no imaginary frequencies were found in the re-optimized structure of $\text{Li}_2[\text{ZnBr}_4]$, which nearly quantitatively preserved the same geometry (only Li-Br bond length differed by 0.02 Å; both structures are included in the supporting ZIP archive).

It should be noted, that a set of computational libraries as libint2³¹ and XCFun (version 0.99)³² are included in the ORCA code (version 4.0.1) to perform the computations efficiently.

2. Energetics of the Elementary Steps

A complete list of the computed energies and transformation Gibbs free energies is given in this section. NHC denotes the 1,3-diisopropylimidazol-2-ylidene ligand throughout this Supporting Information file. All energy values are in kcal/mol.

Table S1. Computed at the RI-TPSS-D3(BJ)/def2-SVP-gCP level (free) energies of the **1** → **1'** transformation in THF.

	ΔE_r^a	ΔG_r^a	ΔG_r^b
M = Ni; L = PMe ₃	-27.1	-6.5	-3.5
M = Ni; L = PMe ₃	-33.1	-9.4	-6.4

^a with the THF concentration correction term added (Equation (2) in the Computational Details section of the main text); ^b no THF concentration correction applied (the Gibbs free energy of an isolated THF molecule was calculated via Equation (1) in the Computational Details section of the main text).

Table S2. Computed at the B97-3c level (free) energies of the **1** → **1'** transformation in THF.

	ΔE_r^a	ΔG_r^a	ΔG_r^b
M = Ni; L = PMe ₃	-15.9	4.9	7.9
M = Ni; L = PMe ₃	-25.0	-1.8	1.1

^a with the THF concentration correction term added (Equation (2) in the Computational Details section of the main text); ^b no THF concentration correction applied (the Gibbs free energy of an isolated THF molecule was calculated via Equation (1) in the Computational Details section of the main text).

2.1. RI-TPSS-D3(BJ)/def2-SVP-gCP, X = Cl

Table S3. Computed (free) energies of the **1** → **4a-e** transformations in THF.

Formed intermediate	ΔE_r	ΔG_r
<i>M = Ni</i>		
4a ; L = PMe ₃	-44.5	-29.4
4c ; L = PMe ₃	-49.3	-33.6
4d ; L = PMe ₃	-51.0	-35.5
4a ; L = PPh ₃	-46.5	-29.5
4e ; L = PPh ₃	-34.5	-29.6
<i>M = Pd</i>		
4b ; L = PMe ₃	-17.0	-13.3
4a ; L = PMe ₃	-20.5	-8.6
4a ; L = PPh ₃	-28.8	-14.3
4d ; L = PPh ₃	-25.3	-8.7

Table S4. Computed (free) energies of the **1** → **2a** and **8** → **9a** transformations in THF.

Formed intermediate	ΔE_r	ΔG_r
<i>M = Ni</i>		
9a ; L ₁ = NHC; L ₂ = THF	-90.0	-66.1
2a ; L = PMe ₃	-77.3	-63.8
2a ; L = PPh ₃	-62.8	-48.5
<i>M = Pd</i>		
9a ; L ₁ = NHC; L ₂ = THF	-58.3	-35.2
2a ; L = PMe ₃	-43.8	-30.5
2a ; L = PPh ₃	-42.4	-27.7

Table S5. Computed (free) energies of the **2a** → **2b** and **9a** → **9b** transformations in THF.

Formed intermediate	ΔE_r	ΔG_r
<i>M = Ni</i>		
9b ; L ₁ = NHC; L ₂ = THF	-12.6	-11.5
9b ; L ₁ = L ₂ = NHC	-8.2	-8.2
2b ; L = PMe ₃	-9.0	-8.3
2b ; L = PPh ₃	-7.1	-6.8
<i>M = Pd</i>		
9b ; L ₁ = NHC; L ₂ = THF	-12.2	-10.8
9b ; L ₁ = L ₂ = NHC	-8.2	-8.4
2b ; L = PMe ₃	-6.2	-6.1
2b ; L = PPh ₃	-4.9	-4.9

Table S6. Computed (free) energies of the **9a** → **9c** and **9c** → **9b** transformations in THF.

Formed intermediate	ΔE_r	ΔG_r
<i>M = Ni</i>		
9a → 9c ; L ₁ = NHC; L ₂ = THF	-8.1	-7.5
9c → 9b ; L ₁ = NHC; L ₂ = THF	-4.5	-4.1
<i>M = Pd</i>		
9a → 9c ; L ₁ = NHC; L ₂ = THF	-11.8	-10.5
9c → 9b ; L ₁ = NHC; L ₂ = THF	-0.3	-0.3

Table S7. Computed (free) energies of the **9a-c** dimerization in THF.

Dimerization reaction	ΔE_r	ΔG_r
<i>M = Ni</i>		
2(THF)[PhNiCl](NHC) (9a) \rightarrow (NHC)[PhNi(μ_2 -Cl)] ₂ (NHC) (14) + 2THF	-28.5	-34.9
2(THF)[PhNiCl](NHC) (9b) \rightarrow (NHC)[PhNi(μ_2 -Cl)] ₂ (NHC) (14) + 2THF	-3.3	-11.8
2(THF)[PhNiCl](NHC) (9c) \rightarrow (NHC)[PhNi(μ_2 -Cl)] ₂ (NHC) (14) + 2THF	-12.3	-20.0
<i>M = Pd</i>		
2(THF)[PhPdCl](NHC) (9a) \rightarrow (NHC)[PhPd(μ_2 -Cl)] ₂ (NHC) (14) + 2THF	-29.5	-35.7
2(THF)[PhPdCl](NHC) (9b) \rightarrow (NHC)[PhPd(μ_2 -Cl)] ₂ (NHC) (14) + 2THF	-5.1	-14.2
2(THF)[PhPdCl](NHC) (9c) \rightarrow (NHC)[PhPd(μ_2 -Cl)] ₂ (NHC) (14) + 2THF	-5.8	-14.7

Table S8. Computed (free) energies of the competing **2a** \rightarrow **6a** and **2a** \rightarrow **5a** transformations (and **9a** \rightarrow **12a** vs. **9a** \rightarrow **11a**) in THF.

Formed intermediate	ΔE_r	ΔG_r	ΔE_r	ΔG_r	Formed intermediate
2a \rightarrow 6a or 9a \rightarrow 12a			2a \rightarrow 5a or 9a \rightarrow 11a		
<i>M = Ni</i>			<i>M = Ni</i>		
12a ; L ₁ = NHC; L ₂ = THF	-4.9	-2.9	-3.0	-0.7	11a ; L ₁ = NHC; L ₂ = THF
12a ; L ₁ = L ₂ = NHC	-7.9	-5.4	-6.8	-4.0	11a ; L ₁ = L ₂ = NHC
6a ; L = PMe ₃	-8.4	-5.5	-5.9	-2.5	5a ; L = PMe ₃
6a ; L = PPh ₃	-6.7	-3.7	-4.5	-0.6	5a ; L = PPh ₃
<i>M = Pd</i>			<i>M = Pd</i>		
12a ; L ₁ = NHC; L ₂ = THF	-2.6	-0.4	-0.9	2.2	11a ; L ₁ = NHC; L ₂ = THF
12a ; L ₁ = L ₂ = NHC	-6.5	-4.1	-5.0	-2.3	11a ; L ₁ = L ₂ = NHC
6a ; L = PMe ₃	-9.6	-7.0	-5.7	-3.2	5a ; L = PMe ₃
6a ; L = PPh ₃	-10.3	-6.4	-1.7	1.3	5a ; L = PPh ₃

Table S9. Computed (free) energies of the **7** (**13**) formation from the intermediates **2a** and **6a** (**9a** and **12a**) in THF.

Formed intermediate	ΔE_r	ΔG_r^a	ΔG_r^b	ΔE_r	ΔG_r^a	ΔG_r^b
	6a \rightarrow 7 or 12a \rightarrow 13			2a \rightarrow 7 or 9a \rightarrow 13		
	<i>M = Ni</i>			<i>M = Ni</i>		
13 ; L ₁ = NHC; L ₂ = THF	13.1	2.7	1.2	8.2	-0.2	-3.2
13 ; L ₁ = L ₂ = NHC	16.5	5.9	4.4	8.6	0.5	-2.4
7 ; L = PMe ₃	13.7	3.5	2.0	5.3	-2.1	-5.0
7 ; L = PPh ₃	13.5	2.8	1.3	6.8	-0.9	-3.9
	<i>M = Pd</i>			<i>M = Pd</i>		
13 ; L ₁ = NHC; L ₂ = THF	10.2	0.6	-0.9	7.6	0.2	-2.8
13 ; L ₁ = L ₂ = NHC	12.6	1.9	0.4	6.0	-2.2	-5.2
7 ; L = PMe ₃	15.7	4.9	3.4	6.1	-2.1	-5.1
7 ; L = PPh ₃	15.1	4.2	2.7	4.8	-2.3	-5.2

^a with the THF concentration correction term added (Equation (2) in the Computational Details section of the main text); ^b no THF concentration correction applied (the Gibbs free energy of an isolated THF molecule was calculated via Equation (1) in the Computational Details section of the main text).

Table S10. Computed (free) energies of the competing **2b** \rightarrow **6b** and **2b** \rightarrow **5b** transformations (and **9b** \rightarrow **12b** vs. **9b** \rightarrow **11b**) in THF.

Formed intermediate	ΔE_r	ΔG_r	ΔE_r	ΔG_r	Formed intermediate
2b \rightarrow 6b or 9b \rightarrow 12b			2b \rightarrow 5b or 9b \rightarrow 11b		
	<i>M = Ni</i>		<i>M = Ni</i>		
12b ; L ₁ = NHC; L ₂ = THF	-6.5	-4.5	-4.2	-2.2	11b ; L ₁ = NHC; L ₂ = THF
12b ; L ₁ = L ₂ = NHC	-7.8	-5.0	-5.2	-2.0	11b ; L ₁ = L ₂ = NHC
6b ; L = PMe ₃	-9.0	-6.1	-5.8	-2.5	5b ; L = PMe ₃
6b ; L = PPh ₃	-6.4	-2.3	-0.6	2.1	5b ; L = PPh ₃
	<i>M = Pd</i>		<i>M = Pd</i>		
12b ; L ₁ = NHC; L ₂ = THF	-8.0	-5.0	-4.3	-1.1	11b ; L ₁ = NHC; L ₂ = THF
12b ; L ₁ = L ₂ = NHC	-9.7	-6.6	-6.7	-3.2	11b ; L ₁ = L ₂ = NHC
6b ; L = PMe ₃	-12.7	-9.6	-8.2	-5.1	5b ; L = PMe ₃
6b ; L = PPh ₃	-8.0	-3.3	-4.9	-1.5	5b ; L = PPh ₃

2.2. RI-TPSS-D3(BJ)/def2-SVP-gCP, X = Br

Table S11. Computed (free) energies of the **1** → **4a-e** transformations in THF.

Formed intermediate	ΔE_r	ΔG_r
<i>M = Ni</i>		
4a ; L = PMe ₃	*	*
4c ; L = PMe ₃	-47.4	-32.2
4d ; L = PMe ₃	-51.5	-36.7
4a ; L = PPh ₃	-42.4	-26.4
4e ; L = PPh ₃	-33.8	-28.8
<i>M = Pd</i>		
4b ; L = PMe ₃	-14.3	-11.3
4a ; L = PMe ₃	-16.7	-2.7
4a ; L = PPh ₃	-24.4	-8.8
4d ; L = PPh ₃	-23.9	-7.2

* The starting **4a**-like structure relaxed to **4c**.

Table S12. Computed (free) energies of the **1** → **2a** and **8** → **9a** transformations in THF.

Formed intermediate	ΔE_r	ΔG_r
<i>M = Ni</i>		
9a ; L ₁ = NHC; L ₂ = THF	-91.2	-67.1
2a ; L = PMe ₃	-79.9	-65.1
2a ; L = PPh ₃	-64.4	-49.3
<i>M = Pd</i>		
9a ; L ₁ = NHC; L ₂ = THF	-60.4	-36.9
2a ; L = PMe ₃	-46.4	-32.9
2a ; L = PPh ₃	-44.9	-30.0

Table S13. Computed (free) energies of the **2a** → **2b** and **9a** → **9b** transformations in THF.

Formed intermediate	ΔE_r	ΔG_r
<i>M = Ni</i>		
9b ; L ₁ = NHC; L ₂ = THF	-11.8	-11.5
9b ; L ₁ = L ₂ = NHC	-8.2	-8.2
2b ; L = PMe ₃	-8.1	-8.5
2b ; L = PPh ₃	-4.6	-4.8
<i>M = Pd</i>		
9b ; L ₁ = NHC; L ₂ = THF	-12.0	-11.0
9b ; L ₁ = L ₂ = NHC	-8.5	-8.6
2b ; L = PMe ₃	-6.5	-6.1
2b ; L = PPh ₃	-1.6	-1.8

Table S14. Computed (free) energies of the **9a** → **9c** and **9c** → **9b** transformations in THF.

Formed intermediate	ΔE_r	ΔG_r
<i>M = Ni</i>		
9a → 9c ; L ₁ = NHC; L ₂ = THF	-7.4	-7.2
9c → 9b ; L ₁ = NHC; L ₂ = THF	-4.4	-4.3
<i>M = Pd</i>		
9a → 9c ; L ₁ = NHC; L ₂ = THF	-11.0	-9.7
9c → 9b ; L ₁ = NHC; L ₂ = THF	-1.0	-1.3

Table S15. Computed (free) energies of the **2a** and **9a** dimerization in THF.

Dimerization reaction	ΔE_r	ΔG_r
<i>M = Ni</i>		
$2(\text{THF})[\text{PhNiBr}](\text{NHC})$ (9a) \rightarrow $(\text{NHC})[\text{PhNi}(\mu_2\text{-Br})_2](\text{NHC})$ (14) + 2THF	-22.0	-28.3
$2\text{Me}_3\text{P}[\text{PhNiBr}]\text{PMe}_3$ (2a) \rightarrow $\text{Me}_3\text{P}[\text{PhNi}(\mu_2\text{-Br})_2]\text{PMe}_3$ + 2PMe ₃	25.2	12.2
$2\text{Ph}_3\text{P}[\text{PhNiBr}]\text{PPh}_3$ (2a) \rightarrow $\text{Ph}_3\text{P}[\text{PhNi}(\mu_2\text{-Br})_2]\text{PPh}_3$ + 2PPh ₃	23.3	8.5
<i>M = Pd</i>		
$2(\text{THF})[\text{PhPdBr}](\text{NHC})$ (9a) \rightarrow $(\text{NHC})[\text{PhPd}(\mu_2\text{-Br})_2](\text{NHC})$ (14) + 2THF	-23.9	-29.9
$2\text{Me}_3\text{P}[\text{PhPdBr}]\text{PMe}_3$ (2a) \rightarrow $\text{Me}_3\text{P}[\text{PhPd}(\mu_2\text{-Br})_2]\text{PMe}_3$ + 2PMe ₃	27.2	16.1
$2\text{Ph}_3\text{P}[\text{PhPdBr}]\text{PPh}_3$ (2a) \rightarrow $\text{Ph}_3\text{P}[\text{PhPd}(\mu_2\text{-Br})_2]\text{PPh}_3$ + 2PPh ₃	28.4	12.5

Table S16. Computed (free) energies of the **2b** and **9b** dimerization in THF.

Dimerization reaction	ΔE_r	ΔG_r
<i>M = Ni</i>		
$2(\text{THF})[\text{PhNiBr}](\text{NHC})$ (9b) \rightarrow $(\text{NHC})[\text{PhNi}(\mu_2\text{-Br})_2](\text{NHC})$ (14) + 2THF	1.5	-5.4
$2\text{Me}_3\text{P}[\text{PhNiBr}]\text{PMe}_3$ (2b) \rightarrow $\text{Me}_3\text{P}[\text{PhNi}(\mu_2\text{-Br})_2]\text{PMe}_3$ + 2PMe ₃	41.4	29.2
$2\text{Ph}_3\text{P}[\text{PhNiBr}]\text{PPh}_3$ (2b) \rightarrow $\text{Ph}_3\text{P}[\text{PhNi}(\mu_2\text{-Br})_2]\text{PPh}_3$ + 2PPh ₃	32.5	18.1
<i>M = Pd</i>		
$2(\text{THF})[\text{PhPdBr}](\text{NHC})$ (9b) \rightarrow $(\text{NHC})[\text{PhPd}(\mu_2\text{-Br})_2](\text{NHC})$ (14) + 2THF	0.1	-7.9
$2\text{Me}_3\text{P}[\text{PhPdBr}]\text{PMe}_3$ (2b) \rightarrow $\text{Me}_3\text{P}[\text{PhPd}(\mu_2\text{-Br})_2]\text{PMe}_3$ + 2PMe ₃	40.2	28.4
$2\text{Ph}_3\text{P}[\text{PhPdBr}]\text{PPh}_3$ (2b) \rightarrow $\text{Ph}_3\text{P}[\text{PhPd}(\mu_2\text{-Br})_2]\text{PPh}_3$ + 2PPh ₃	31.6	16.1

Table S17. Computed (free) energies of the **9c** dimerization in THF.

Dimerization reaction	ΔE_r	ΔG_r
<i>M = Ni</i>		
2(THF)[PhNiBr](NHC) (9c) \rightarrow (NHC)[PhNi(μ_2 -Br)] ₂ (NHC) (14) + 2THF	-7.3	-14.0
<i>M = Pd</i>		
2(THF)[PhPdBr](NHC) (9c) \rightarrow (NHC)[PhPd(μ_2 -Br)] ₂ (NHC) (14) + 2THF	-2.0	-10.5

Table S18. Computed (free) energies of the competing **2a** \rightarrow **6a** and **2a** \rightarrow **5a** transformations (and **9a** \rightarrow **12a** vs. **9a** \rightarrow **11a**) in THF.

Formed intermediate	ΔE_r	ΔG_r	ΔE_r	ΔG_r	Formed intermediate
2a \rightarrow 6a or 9a \rightarrow 12a			2a \rightarrow 5a or 9a \rightarrow 11a		
<i>M = Ni</i>			<i>M = Ni</i>		
12a ; L ₁ = NHC; L ₂ = THF	-1.1	0.7	-1.5	1.8	11a ; L ₁ = NHC; L ₂ = THF
12a ; L ₁ = L ₂ = NHC	-4.3	-0.9	-3.7	0.6	11a ; L ₁ = L ₂ = NHC
6a ; L = PMe ₃	-4.5	-2.2	-3.1	0.2	5a ; L = PMe ₃
6a ; L = PPh ₃	-3.4	0.0	-2.5	1.9	5a ; L = PPh ₃
<i>M = Pd</i>			<i>M = Pd</i>		
12a ; L ₁ = NHC; L ₂ = THF	0.3	3.6	1.3	5.6	11a ; L ₁ = NHC; L ₂ = THF
12a ; L ₁ = L ₂ = NHC	-3.4	0.8	-2.1	2.1	11a ; L ₁ = L ₂ = NHC
6a ; L = PMe ₃	-5.4	-2.0	-2.0	3.0	5a ; L = PMe ₃
6a ; L = PPh ₃	-5.5	-1.5	-0.8	4.7	5a ; L = PPh ₃

Table S19. Computed (free) energies of the **7** (**13**) formation from the intermediates **2a** and **6a** (**9a** and **12a**) in THF.

Formed intermediate	ΔE_r	ΔG_r^a	ΔG_r^b	ΔE_r	ΔG_r^a	ΔG_r^b
	6a \rightarrow 7 or 12a \rightarrow 13			2a \rightarrow 7 or 9a \rightarrow 13		
	<i>M</i> = <i>Ni</i>			<i>M</i> = <i>Ni</i>		
13 ; L ₁ = NHC; L ₂ = THF	7.8	-1.7	-3.2	6.8	-0.9	-3.9
13 ; L ₁ = L ₂ = NHC	12.4	1.5	0.0	8.2	0.6	-2.4
7 ; L = PMe ₃	10.4	0.4	-1.1	5.9	-1.8	-4.8
7 ; L = PPh ₃	9.5	-1.0	-2.5	6.1	-1.1	-4.1
	<i>M</i> = <i>Pd</i>			<i>M</i> = <i>Pd</i>		
13 ; L ₁ = NHC; L ₂ = THF	8.8	-1.5	-3.0	9.1	2.1	-0.9
13 ; L ₁ = L ₂ = NHC	9.0	-2.4	-3.9	5.6	-1.7	-4.7
7 ; L = PMe ₃	11.6	0.6	-0.8	6.2	-1.4	-4.4
7 ; L = PPh ₃	11.4	0.7	-0.8	5.9	-0.9	-3.9

^a with the THF concentration correction term added (Equation (2) in the Computational Details section of the main text); ^b no THF concentration correction applied (the Gibbs free energy of an isolated THF molecule was calculated via Equation (1) in the Computational Details section of the main text).

Table S20. Computed (free) energies of the competing **2b** \rightarrow **6b** and **2b** \rightarrow **5b** transformations (and **9b** \rightarrow **12b** vs. **9b** \rightarrow **11b**) in THF.

Formed intermediate	ΔE_r	ΔG_r	ΔE_r	ΔG_r	Formed intermediate
	2b \rightarrow 6b or 9b \rightarrow 12b		2b \rightarrow 5b or 9b \rightarrow 11b		
	<i>M</i> = <i>Ni</i>		<i>M</i> = <i>Ni</i>		
12b ; L ₁ = NHC; L ₂ = THF	-3.8	-1.0	-0.2	3.7	11b ; L ₁ = NHC; L ₂ = THF
12b ; L ₁ = L ₂ = NHC	-3.1	-0.1	-0.9	3.2	11b ; L ₁ = L ₂ = NHC
6b ; L = PMe ₃	-3.1	0.0	-1.5	2.4	5b ; L = PMe ₃
6b ; L = PPh ₃	-6.1	-1.4	0.7	5.1	5b ; L = PPh ₃
	<i>M</i> = <i>Pd</i>		<i>M</i> = <i>Pd</i>		
12b ; L ₁ = NHC; L ₂ = THF	-1.4	2.4	-0.8	3.9	11b ; L ₁ = NHC; L ₂ = THF
12b ; L ₁ = L ₂ = NHC	-4.4	-0.8	-2.6	1.9	11b ; L ₁ = L ₂ = NHC
6b ; L = PMe ₃	-6.0	-3.2	2.4	6.8	5b ; L = PMe ₃
6b ; L = PPh ₃	-7.5	-3.1	-0.7	4.0	5b ; L = PPh ₃

2.3. RI-TPSS-D3(BJ)/def2-SVP-gCP, X = I

Table S21. Computed (free) energies of the **1** → **4a-e** transformations in THF.

Formed intermediate	ΔE_r	ΔG_r
<i>M = Ni</i>		
4a ; L = PMe ₃	*	*
4c ; L = PMe ₃	-48.1	-32.0
4d ; L = PMe ₃	-51.5	-36.0
4a ; L = PPh ₃	-42.8	-24.0
4e ; L = PPh ₃	-34.4	-27.9
<i>M = Pd</i>		
4b ; L = PMe ₃	-13.0	-9.5
4a ; L = PMe ₃	-17.8	-3.5
4a ; L = PPh ₃	-26.8	-10.3
4d ; L = PPh ₃	-25.8	-7.7

* The starting **4a**-like structure relaxed to **4c**.Table S22. Computed (free) energies of the **1** → **2a** and **8** → **9a** transformations in THF.

Formed intermediate	ΔE_r	ΔG_r
<i>M = Ni</i>		
9a ; L ₁ = NHC; L ₂ = THF	-92.9	-68.6
2a ; L = PMe ₃	-80.5	-66.3
2a ; L = PPh ₃	-67.9	-52.7
<i>M = Pd</i>		
9a ; L ₁ = NHC; L ₂ = THF	-63.4	-39.6
2a ; L = PMe ₃	-47.5	-33.7
2a ; L = PPh ₃	-46.9	-31.7

Table S23. Computed (free) energies of the **2a** → **2b** and **9a** → **9b** transformations in THF.

Formed intermediate	ΔE_r	ΔG_r
<i>M = Ni</i>		
9b ; L ₁ = NHC; L ₂ = THF	-13.0	-12.3
9b ; L ₁ = L ₂ = NHC	-8.4	-8.4
2b ; L = PMe ₃	-7.6	-7.3
2b ; L = PPh ₃	-0.2	0.0
<i>M = Pd</i>		
9b ; L ₁ = NHC; L ₂ = THF	-10.6	-9.5
9b ; L ₁ = L ₂ = NHC	-9.2	-9.3
2b ; L = PMe ₃	-7.3	-6.8
2b ; L = PPh ₃	-0.9	-1.0

Table S24. Computed (free) energies of the **9a** → **9c** and **9c** → **9b** transformations in THF.

Formed intermediate	ΔE_r	ΔG_r
<i>M = Ni</i>		
9a → 9c ; L ₁ = NHC; L ₂ = THF	-6.4	-5.9
9c → 9b ; L ₁ = NHC; L ₂ = THF	-6.7	-6.3
<i>M = Pd</i>		
9a → 9c ; L ₁ = NHC; L ₂ = THF	-8.7	-7.6
9c → 9b ; L ₁ = NHC; L ₂ = THF	-1.9	-1.9

Table S25. Computed (free) energies of the **9a-c** dimerization in THF.

Dimerization reaction	ΔE_r	ΔG_r
<i>M = Ni</i>		
2(THF)[PhNiI](NHC) (9a) \rightarrow (NHC)[PhNi(μ_2 -I)] ₂ (NHC) (14) + 2THF	-16.1	-22.4
2(THF)[PhNiI](NHC) (9b) \rightarrow (NHC)[PhNi(μ_2 -I)] ₂ (NHC) (14) + 2THF	9.9	2.1
2(THF)[PhNiI](NHC) (9c) \rightarrow (NHC)[PhNi(μ_2 -I)] ₂ (NHC) (14) + 2THF	-3.4	-10.6
<i>M = Pd</i>		
2(THF)[PhPdI](NHC) (9a) \rightarrow (NHC)[PhPd(μ_2 -I)] ₂ (NHC) (14) + 2THF	-19.8	-25.5
2(THF)[PhPdI](NHC) (9b) \rightarrow (NHC)[PhPd(μ_2 -I)] ₂ (NHC) (14) + 2THF	1.5	-6.5
2(THF)[PhPdI](NHC) (9c) \rightarrow (NHC)[PhPd(μ_2 -I)] ₂ (NHC) (14) + 2THF	-2.3	-10.2

Table S26. Computed (free) energies of the competing **2a** \rightarrow **6a** and **2a** \rightarrow **5a** transformations (and **9a** \rightarrow **12a** vs. **9a** \rightarrow **11a**) in THF.

Formed intermediate	ΔE_r	ΔG_r	ΔE_r	ΔG_r	Formed intermediate
2a \rightarrow 6a or 9a \rightarrow 12a			2a \rightarrow 5a or 9a \rightarrow 11a		
	<i>M = Ni</i>		<i>M = Ni</i>		
12a ; L ₁ = NHC; L ₂ = THF	0.1	3.6	-1.3	2.4	11a ; L ₁ = NHC; L ₂ = THF
12a ; L ₁ = L ₂ = NHC	-1.4	2.2	-3.1	1.1	11a ; L ₁ = L ₂ = NHC
6a ; L = PMe ₃	-1.4	3.2	-2.7	2.0	5a ; L = PMe ₃
6a ; L = PPh ₃	1.1	5.4	0.1	6.1	5a ; L = PPh ₃
	<i>M = Pd</i>		<i>M = Pd</i>		
12a ; L ₁ = NHC; L ₂ = THF	2.1	5.9	0.7	5.1	11a ; L ₁ = NHC; L ₂ = THF
12a ; L ₁ = L ₂ = NHC	-0.6	3.1	-2.1	1.9	11a ; L ₁ = L ₂ = NHC
6a ; L = PMe ₃	-3.5	0.4	-3.5	0.7	5a ; L = PMe ₃
6a ; L = PPh ₃	-2.8	2.8	-1.0	4.1	5a ; L = PPh ₃

Table S27. Computed (free) energies of the **7** (**13**) formation from the intermediates **2a** and **6a** (**9a** and **12a**) in THF.

Formed intermediate	ΔE_r	ΔG_r^a	ΔG_r^b	ΔE_r	ΔG_r^a	ΔG_r^b
	6a \rightarrow 7 or 12a \rightarrow 13			2a \rightarrow 7 or 9a \rightarrow 13		
	<i>M</i> = <i>Ni</i>			<i>M</i> = <i>Ni</i>		
13 ; L ₁ = NHC; L ₂ = THF	9.0	-1.4	-2.9	9.2	2.2	-0.8
13 ; L ₁ = L ₂ = NHC	13.2	2.6	1.1	11.8	4.8	1.8
7 ; L = PMe ₃	9.1	-1.2	-2.7	7.8	1.9	-1.0
7 ; L = PPh ₃	9.5	-0.5	-2.0	10.6	4.9	1.9
	<i>M</i> = <i>Pd</i>			<i>M</i> = <i>Pd</i>		
13 ; L ₁ = NHC; L ₂ = THF	9.7	-1.1	-2.6	11.8	4.7	1.8
13 ; L ₁ = L ₂ = NHC	8.7	-1.8	-3.3	8.1	1.3	-1.7
7 ; L = PMe ₃	10.5	0.1	-1.4	7.1	0.5	-2.5
7 ; L = PPh ₃	10.3	-0.9	-2.3	7.5	2.0	-1.0

^a with the THF concentration correction term added (Equation (2) in the Computational Details section of the main text); ^b no THF concentration correction applied (the Gibbs free energy of an isolated THF molecule was calculated via Equation (1) in the Computational Details section of the main text).

Table S28. Computed (free) energies of the competing **2b** \rightarrow **6b** and **2b** \rightarrow **5b** transformations (and **9b** \rightarrow **12b** vs. **9b** \rightarrow **11b**) in THF.

Formed intermediate	ΔE_r	ΔG_r	ΔE_r	ΔG_r	Formed intermediate
2b \rightarrow 6b or 9b \rightarrow 12b			2b \rightarrow 5b or 9b \rightarrow 11b		
	<i>M</i> = <i>Ni</i>		<i>M</i> = <i>Ni</i>		
12b ; L ₁ = NHC; L ₂ = THF	0.4	4.0	0.0	3.9	11b ; L ₁ = NHC; L ₂ = THF
12b ; L ₁ = L ₂ = NHC	0.0	3.6	-1.2	2.9	11b ; L ₁ = L ₂ = NHC
6b ; L = PMe ₃	-1.5	2.5	-1.5	2.1	5b ; L = PMe ₃
6b ; L = PPh ₃	-3.8	0.8	-0.9	3.6	5b ; L = PPh ₃
	<i>M</i> = <i>Pd</i>		<i>M</i> = <i>Pd</i>		
12b ; L ₁ = NHC; L ₂ = THF	1.5	5.8	-1.1	3.0	11b ; L ₁ = NHC; L ₂ = THF
12b ; L ₁ = L ₂ = NHC	-1.7	2.7	-2.6	1.9	11b ; L ₁ = L ₂ = NHC
6b ; L = PMe ₃	-1.3	1.6	-2.4	1.8	5b ; L = PMe ₃
6b ; L = PPh ₃	-3.4	1.5	-1.4	3.1	5b ; L = PPh ₃

2.4. B97-3c, X = Cl

Table S29. Computed (free) energies of the **1** → **4a-e** transformations in THF.

Formed intermediate	ΔE_r	ΔG_r
<i>M = Ni</i>		
4a ; L = PMe ₃	*	*
4c ; L = PMe ₃	-34.2	-20.0
4d ; L = PMe ₃	-42.0	-27.7
4a ; L = PPh ₃	-34.7	-18.1
4e ; L = PPh ₃	-23.7	-19.4
<i>M = Pd</i>		
4b ; L = PMe ₃	-14.9	-11.5
4a ; L = PMe ₃	**	**
4a ; L = PPh ₃	-20.4	-5.1
4d ; L = PPh ₃	-2.5	14.5

* The starting **4a**-like structure relaxed to **4c**; ** the starting **4a**-like structure relaxed to **4b**.

Table S30. Computed (free) energies of the **1** → **2a** and **8** → **9a** transformations in THF.

Formed intermediate	ΔE_r	ΔG_r
<i>M = Ni</i>		
9a ; L ₁ = NHC; L ₂ = THF	-76.2	-52.2
2a ; L = PMe ₃	-60.4	-46.8
2a ; L = PPh ₃	-43.1	-28.2
<i>M = Pd</i>		
9a ; L ₁ = NHC; L ₂ = THF	-50.8	-27.1
2a ; L = PMe ₃	-38.8	-25.5
2a ; L = PPh ₃	-36.2	-21.2

Table S31. Computed (free) energies of the **2a** → **2b** and **9a** → **9b** transformations in THF.

Formed intermediate	ΔE_r	ΔG_r
<i>M = Ni</i>		
9b ; L ₁ = NHC; L ₂ = THF	-12.9	-11.9
9b ; L ₁ = L ₂ = NHC	-14.5	-14.2
2b ; L = PMe ₃	-8.6	-8.1
2b ; L = PPh ₃	-7.4	-7.5
<i>M = Pd</i>		
9b ; L ₁ = NHC; L ₂ = THF	-13.8	-13.2
9b ; L ₁ = L ₂ = NHC	-6.8	-7.2
2b ; L = PMe ₃	-7.8	-7.3
2b ; L = PPh ₃	-3.5	-3.9

Table S32. Computed (free) energies of the **9a** → **9c** and **9c** → **9b** transformations in THF.

Formed intermediate	ΔE_r	ΔG_r
<i>M = Ni</i>		
9a → 9c ; L ₁ = NHC; L ₂ = THF	-8.8	-8.3
9c → 9b ; L ₁ = NHC; L ₂ = THF	-4.1	-3.6
<i>M = Pd</i>		
9a → 9c ; L ₁ = NHC; L ₂ = THF	-13.9	-13.0
9c → 9b ; L ₁ = NHC; L ₂ = THF	0.1	-0.2

Table S33. Computed (free) energies of the **9a-c** dimerization in THF.

Dimerization reaction	ΔE_r	ΔG_r
<i>M = Ni</i>		
2(THF)[PhNiCl](NHC) (9a) \rightarrow (NHC)[PhNi(μ_2 -Cl)] ₂ (NHC) (14) + 2THF	-26.5	-32.8
2(THF)[PhNiCl](NHC) (9b) \rightarrow (NHC)[PhNi(μ_2 -Cl)] ₂ (NHC) (14) + 2THF	-0.6	-9.0
2(THF)[PhNiCl](NHC) (9c) \rightarrow (NHC)[PhNi(μ_2 -Cl)] ₂ (NHC) (14) + 2THF	-8.9	-16.2
<i>M = Pd</i>		
2(THF)[PhPdCl](NHC) (9a) \rightarrow (NHC)[PhPd(μ_2 -Cl)] ₂ (NHC) (14) + 2THF	-30.7	-37.6
2(THF)[PhPdCl](NHC) (9b) \rightarrow (NHC)[PhPd(μ_2 -Cl)] ₂ (NHC) (14) + 2THF	-3.0	-11.2
2(THF)[PhPdCl](NHC) (9c) \rightarrow (NHC)[PhPd(μ_2 -Cl)] ₂ (NHC) (14) + 2THF	-2.9	-11.6

Table S34. Computed (free) energies of the competing **2a** \rightarrow **6a** and **2a** \rightarrow **5a** transformations (and **9a** \rightarrow **12a** vs. **9a** \rightarrow **11a**) in THF.

Formed intermediate	ΔE_r	ΔG_r	ΔE_r	ΔG_r	Formed intermediate
2a \rightarrow 6a or 9a \rightarrow 12a			2a \rightarrow 5a or 9a \rightarrow 11a		
	<i>M = Ni</i>		<i>M = Ni</i>		
12a ; L ₁ = NHC; L ₂ = THF	-3.8	-1.1	-2.5	-0.3	11a ; L ₁ = NHC; L ₂ = THF
12a ; L ₁ = L ₂ = NHC	-7.1	-4.1	-6.2	-2.8	11a ; L ₁ = L ₂ = NHC
6a ; L = PMe ₃	-6.4	-2.8	-3.8	-0.2	5a ; L = PMe ₃
6a ; L = PPh ₃	-11.2	-7.7	-9.5	-4.6	5a ; L = PPh ₃
	<i>M = Pd</i>		<i>M = Pd</i>		
12a ; L ₁ = NHC; L ₂ = THF	-4.2	-1.3	-1.1	1.6	11a ; L ₁ = NHC; L ₂ = THF
12a ; L ₁ = L ₂ = NHC	-6.5	-3.8	-5.3	-2.2	11a ; L ₁ = L ₂ = NHC
6a ; L = PMe ₃	-7.4	-4.8	-6.1	-2.7	5a ; L = PMe ₃
6a ; L = PPh ₃	-7.6	-4.4	-4.3	-0.8	5a ; L = PPh ₃

Table S35. Computed (free) energies of the **7** (**13**) formation from the intermediates **2a** and **6a** (**9a** and **12a**) in THF.

Formed intermediate	ΔE_r	ΔG_r^a	ΔG_r^b	ΔE_r	ΔG_r^a	ΔG_r^b
	6a \rightarrow 7 or 12a \rightarrow 13			2a \rightarrow 7 or 9a \rightarrow 13		
	<i>M</i> = <i>Ni</i>			<i>M</i> = <i>Ni</i>		
13 ; L ₁ = NHC; L ₂ = THF	11.8	1.3	-0.2	8.0	0.2	-2.8
13 ; L ₁ = L ₂ = NHC	11.5	0.6	-0.9	4.4	-3.5	-6.5
7 ; L = PMe ₃	14.3	3.1	1.6	7.9	0.3	-2.6
7 ; L = PPh ₃	13.8	2.9	1.4	2.6	-4.8	-7.8
	<i>M</i> = <i>Pd</i>			<i>M</i> = <i>Pd</i>		
13 ; L ₁ = NHC; L ₂ = THF	11.8	0.9	-0.6	7.6	-0.4	-3.4
13 ; L ₁ = L ₂ = NHC	10.9	0.0	-1.5	4.5	-3.8	-6.7
7 ; L = PMe ₃	13.9	3.2	1.7	6.4	-1.6	-4.6
7 ; L = PPh ₃	13.4	2.7	1.2	5.8	-1.8	-4.8

^a with the THF concentration correction term added (Equation (2) in the Computational Details section of the main text); ^b no THF concentration correction applied (the Gibbs free energy of an isolated THF molecule was calculated via Equation (1) in the Computational Details section of the main text).

Table S36. Computed (free) energies of the competing **2b** \rightarrow **6b** and **2b** \rightarrow **5b** transformations (and **9b** \rightarrow **12b** vs. **9b** \rightarrow **11b**) in THF.

Formed intermediate	ΔE_r	ΔG_r	ΔE_r	ΔG_r	Formed intermediate
2b \rightarrow 6b or 9b \rightarrow 12b			2b \rightarrow 5b or 9b \rightarrow 11b		
	<i>M</i> = <i>Ni</i>		<i>M</i> = <i>Ni</i>		
12b ; L ₁ = NHC; L ₂ = THF	-7.3	-3.7	-3.7	-0.6	11b ; L ₁ = NHC; L ₂ = THF
12b ; L ₁ = L ₂ = NHC	-2.6	0.5	0.0	4.2	11b ; L ₁ = L ₂ = NHC
6b ; L = PMe ₃	-6.4	-3.0	-5.0	-1.7	5b ; L = PMe ₃
6b ; L = PPh ₃	-10.7	-5.7	-8.5	-3.8	5b ; L = PPh ₃
	<i>M</i> = <i>Pd</i>		<i>M</i> = <i>Pd</i>		
12b ; L ₁ = NHC; L ₂ = THF	-8.1	-4.3	-4.6	-1.0	11b ; L ₁ = NHC; L ₂ = THF
12b ; L ₁ = L ₂ = NHC	-8.5	-4.6	-6.3	-2.4	11b ; L ₁ = L ₂ = NHC
6b ; L = PMe ₃	-9.0	-5.6	-6.7	-2.9	5b ; L = PMe ₃
6b ; L = PPh ₃	-8.4	-4.4	-5.4	-1.4	5b ; L = PPh ₃

2.5. B97-3c, X = Br

Table S37. Computed (free) energies of the **1** → **4a-e** transformations in THF.

Formed intermediate	ΔE_r	ΔG_r
<i>M = Ni</i>		
4a ; L = PMe ₃	*	*
4c ; L = PMe ₃	-37.0	-22.1
4d ; L = PMe ₃	-41.6	-26.7
4a ; L = PPh ₃	-38.9	-21.5
4e ; L = PPh ₃	-26.3	-21.0
<i>M = Pd</i>		
4b ; L = PMe ₃	-15.3	-11.7
4a ; L = PMe ₃	**	**
4a ; L = PPh ₃	-23.5	-7.5
4d ; L = PPh ₃	-22.9	-5.1

* The starting **4a**-like structure relaxed to **4c**; ** the starting **4a**-like structure relaxed to **4b**.

Table S38. Computed (free) energies of the **1** → **2a** and **8** → **9a** transformations in THF.

Formed intermediate	ΔE_r	ΔG_r
<i>M = Ni</i>		
9a ; L ₁ = NHC; L ₂ = THF	-80.2	-55.7
2a ; L = PMe ₃	-63.0	-49.0
2a ; L = PPh ₃	-51.2	-35.7
<i>M = Pd</i>		
9a ; L ₁ = NHC; L ₂ = THF	-54.7	-30.8
2a ; L = PMe ₃	-42.4	-28.9
2a ; L = PPh ₃	-38.5	-23.3

Table S39. Computed (free) energies of the **2a** → **2b** and **9a** → **9b** transformations in THF.

Formed intermediate	ΔE_r	ΔG_r
<i>M = Ni</i>		
9b ; L ₁ = NHC; L ₂ = THF	-11.8	-10.9
9b ; L ₁ = L ₂ = NHC	-9.7	-9.8
2b ; L = PMe ₃	-8.9	-9.0
2b ; L = PPh ₃	-4.5	-4.2
<i>M = Pd</i>		
9b ; L ₁ = NHC; L ₂ = THF	-14.7	-13.7
9b ; L ₁ = L ₂ = NHC	-10.4	-10.8
2b ; L = PMe ₃	-8.1	-7.3
2b ; L = PPh ₃	-3.0	-3.1

Table S40. Computed (free) energies of the **9a** → **9c** and **9c** → **9b** transformations in THF.

Formed intermediate	ΔE_r	ΔG_r
<i>M = Ni</i>		
9a → 9c ; L ₁ = NHC; L ₂ = THF	-7.6	-7.0
9c → 9b ; L ₁ = NHC; L ₂ = THF	-4.2	-3.9
<i>M = Pd</i>		
9a → 9c ; L ₁ = NHC; L ₂ = THF	-13.4	-11.9
9c → 9b ; L ₁ = NHC; L ₂ = THF	-1.4	-1.8

Table S41. Computed (free) energies of the **2a** and **9a** dimerization in THF.

Dimerization reaction	ΔE_r	ΔG_r
<i>M = Ni</i>		
2(THF)[PhNiBr](NHC) (9a) \rightarrow (NHC)[PhNi(μ_2 -Br)] ₂ (NHC) (14) + 2THF	-22.6	-29.0
2Me ₃ P[PhNiBr]PMe ₃ (2a) \rightarrow Me ₃ P[PhNi(μ_2 -Br)] ₂ PMe ₃ + 2PMe ₃	26.6	15.1
2Ph ₃ P[PhNiBr]PPh ₃ (2a) \rightarrow Ph ₃ P[PhNi(μ_2 -Br)] ₂ PPh ₃ + 2PPh ₃	23.0	9.0
<i>M = Pd</i>		
2(THF)[PhPdBr](NHC) (9a) \rightarrow (NHC)[PhPd(μ_2 -Br)] ₂ (NHC) (14) + 2THF	-30.2	-37.2
2Me ₃ P[PhPdBr]PMe ₃ (2a) \rightarrow Me ₃ P[PhPd(μ_2 -Br)] ₂ PMe ₃ + 2PMe ₃	28.7	18.2
2Ph ₃ P[PhPdBr]PPh ₃ (2a) \rightarrow Ph ₃ P[PhPd(μ_2 -Br)] ₂ PPh ₃ + 2PPh ₃	26.7	13.1

Table S42. Computed (free) energies of the **2b** and **9b** dimerization in THF.

Dimerization reaction	ΔE_r	ΔG_r
<i>M = Ni</i>		
2(THF)[PhNiBr](NHC) (9b) \rightarrow (NHC)[PhNi(μ_2 -Br)] ₂ (NHC) (14) + 2THF	0.9	-7.2
2Me ₃ P[PhNiBr]PMe ₃ (2b) \rightarrow Me ₃ P[PhNi(μ_2 -Br)] ₂ PMe ₃ + 2PMe ₃	44.5	33.0
2Ph ₃ P[PhNiBr]PPh ₃ (2b) \rightarrow Ph ₃ P[PhNi(μ_2 -Br)] ₂ PPh ₃ + 2PPh ₃	32.1	17.5
<i>M = Pd</i>		
2(THF)[PhPdBr](NHC) (9b) \rightarrow (NHC)[PhPd(μ_2 -Br)] ₂ (NHC) (14) + 2THF	-0.7	-9.9
2Me ₃ P[PhPdBr]PMe ₃ (2b) \rightarrow Me ₃ P[PhPd(μ_2 -Br)] ₂ PMe ₃ + 2PMe ₃	44.8	32.7
2Ph ₃ P[PhPdBr]PPh ₃ (2b) \rightarrow Ph ₃ P[PhPd(μ_2 -Br)] ₂ PPh ₃ + 2PPh ₃	32.7	19.3

Table S43. Computed (free) energies of the **9c** dimerization in THF.

Dimerization reaction	ΔE_r	ΔG_r
<i>M = Ni</i>		
2(THF)[PhNiBr](NHC) (9c) \rightarrow (NHC)[PhNi(μ_2 -Br)] ₂ (NHC) (14) + 2THF	-7.5	-15.1
<i>M = Pd</i>		
2(THF)[PhPdBr](NHC) (9c) \rightarrow (NHC)[PhPd(μ_2 -Br)] ₂ (NHC) (14) + 2THF	-3.5	-13.4

Table S44. Computed (free) energies of the competing **2a** → **6a** and **2a** → **5a** transformations (and **9a** → **12a** vs. **9a** → **11a**) in THF.

Formed intermediate	ΔE_r	ΔG_r	ΔE_r	ΔG_r	Formed intermediate
2a → 6a or 9a → 12a			2a → 5a or 9a → 11a		
<i>M = Ni</i>			<i>M = Ni</i>		
12a ; L ₁ = NHC; L ₂ = THF	-4.3	-0.9	-1.9	0.8	11a ; L ₁ = NHC; L ₂ = THF
12a ; L ₁ = L ₂ = NHC	-6.7	-3.5	-5.3	-1.4	11a ; L ₁ = L ₂ = NHC
6a ; L = PMe ₃	-7.0	-3.1	-4.1	0.0	5a ; L = PMe ₃
6a ; L = PPh ₃	-6.1	-3.0	-4.5	1.2	5a ; L = PPh ₃
<i>M = Pd</i>			<i>M = Pd</i>		
12a ; L ₁ = NHC; L ₂ = THF	-5.5	-2.0	-2.4	1.7	11a ; L ₁ = NHC; L ₂ = THF
12a ; L ₁ = L ₂ = NHC	-6.2	-2.8	-5.0	-1.1	11a ; L ₁ = L ₂ = NHC
6a ; L = PMe ₃	-7.1	-3.0	-6.5	-2.3	5a ; L = PMe ₃
6a ; L = PPh ₃	-9.8	-5.5	-6.2	-1.2	5a ; L = PPh ₃

Table S45. Computed (free) energies of the **7** (**13**) formation from the intermediates **2a** and **6a** (**9a** and **12a**) in THF.

Formed intermediate	ΔE_r	ΔG_r^a	ΔG_r^b	ΔE_r	ΔG_r^a	ΔG_r^b
6a → 7 or 12a → 13			2a → 7 or 9a → 13			
<i>M = Ni</i>			<i>M = Ni</i>			
13 ; L ₁ = NHC; L ₂ = THF	12.1	1.1	-0.4	7.8	0.2	-2.8
13 ; L ₁ = L ₂ = NHC	11.4	0.6	-0.9	4.8	-2.9	-5.9
7 ; L = PMe ₃	14.5	3.7	2.2	7.4	0.6	-2.4
7 ; L = PPh ₃	11.9	1.4	-0.1	5.7	-1.6	-4.6
<i>M = Pd</i>			<i>M = Pd</i>			
13 ; L ₁ = NHC; L ₂ = THF	13.2	2.4	0.9	7.6	0.4	-2.6
13 ; L ₁ = L ₂ = NHC	8.1	-3.0	-4.5	1.9	-5.9	-8.8
7 ; L = PMe ₃	13.0	1.6	0.1	5.9	-1.4	-4.4
7 ; L = PPh ₃	14.2	2.6	1.2	4.4	-2.9	-5.8

^a with the THF concentration correction term added (Equation (2) in the Computational Details section of the main text); ^b no THF concentration correction applied (the Gibbs free energy of an isolated THF molecule was calculated via Equation (1) in the Computational Details section of the main text).

Table S46. Computed (free) energies of the competing **2b** → **6b** and **2b** → **5b** transformations (and **9b** → **12b** vs. **9b** → **11b**) in THF.

Formed intermediate	ΔE_r	ΔG_r	ΔE_r	ΔG_r	Formed intermediate
2b → 6b or 9b → 12b			2b → 5b or 9b → 11b		
	<i>M = Ni</i>		<i>M = Ni</i>		
12b ; L ₁ = NHC; L ₂ = THF	-5.7	-2.1	-4.5	-0.8	11b ; L ₁ = NHC; L ₂ = THF
12b ; L ₁ = L ₂ = NHC	-7.5	-3.6	-5.3	-0.2	11b ; L ₁ = L ₂ = NHC
6b ; L = PMe ₃	-6.4	-2.1	-4.7	-0.5	5b ; L = PMe ₃
6b ; L = PPh ₃	-8.9	-4.3	-6.2	-1.2	5b ; L = PPh ₃
	<i>M = Pd</i>		<i>M = Pd</i>		
12b ; L ₁ = NHC; L ₂ = THF	-6.1	-2.2	-2.9	1.1	11b ; L ₁ = NHC; L ₂ = THF
12b ; L ₁ = L ₂ = NHC	-8.6	-4.5	-5.8	-1.3	11b ; L ₁ = L ₂ = NHC
6b ; L = PMe ₃	-8.5	-5.1	-6.3	-1.8	5b ; L = PMe ₃
6b ; L = PPh ₃	-11.1	-6.3	-7.6	-2.5	5b ; L = PPh ₃

2.6. B97-3c, X = I

Table S47. Computed (free) energies of the **1** → **4a-e** transformations in THF.

Formed intermediate	ΔE_r	ΔG_r
<i>M = Ni</i>		
4a ; L = PMe ₃	-39.1	-24.7
4c ; L = PMe ₃	-41.2	-26.8
4d ; L = PMe ₃	-44.3	-29.6
4a ; L = PPh ₃	-42.5	-23.8
4e ; L = PPh ₃	-30.0	-23.9
<i>M = Pd</i>		
4b ; L = PMe ₃	-16.7	-12.9
4a ; L = PMe ₃	-21.2	-7.1
4a ; L = PPh ₃	-27.0	-10.3
4d ; L = PPh ₃	-26.2	-8.6

Table S48. Computed (free) energies of the **1** → **2a** and **8** → **9a** transformations in THF.

Formed intermediate	ΔE_r	ΔG_r
<i>M = Ni</i>		
9a ; L ₁ = NHC; L ₂ = THF	-83.2	-58.0
2a ; L = PMe ₃	-66.3	-51.5
2a ; L = PPh ₃	-56.1	-39.5
<i>M = Pd</i>		
9a ; L ₁ = NHC; L ₂ = THF	-59.2	-34.6
2a ; L = PMe ₃	-46.2	-31.7
2a ; L = PPh ₃	-39.3	-23.0

Table S49. Computed (free) energies of the **2a** → **2b** and **9a** → **9b** transformations in THF.

Formed intermediate	ΔE_r	ΔG_r
<i>M = Ni</i>		
9b ; L ₁ = NHC; L ₂ = THF	-10.6	-9.0
9b ; L ₁ = L ₂ = NHC	-15.4	-16.2
2b ; L = PMe ₃	-8.1	-7.7
2b ; L = PPh ₃	-0.1	0.0
<i>M = Pd</i>		
9b ; L ₁ = NHC; L ₂ = THF	-13.2	-12.1
9b ; L ₁ = L ₂ = NHC	-10.9	-11.2
2b ; L = PMe ₃	-7.8	-7.1
2b ; L = PPh ₃	-5.3	-5.6

Table S50. Computed (free) energies of the **9a** → **9c** and **9c** → **9b** transformations in THF.

Formed intermediate	ΔE_r	ΔG_r
<i>M = Ni</i>		
9a → 9c ; L ₁ = NHC; L ₂ = THF	-6.5	-6.0
9c → 9b ; L ₁ = NHC; L ₂ = THF	-4.1	-3.0
<i>M = Pd</i>		
9a → 9c ; L ₁ = NHC; L ₂ = THF	-11.2	-10.2
9c → 9b ; L ₁ = NHC; L ₂ = THF	-2.0	-1.9

Table S51. Computed (free) energies of the **9a-c** dimerization in THF.

Dimerization reaction	ΔE_r	ΔG_r
<i>M = Ni</i>		
2(THF)[PhNiI](NHC) (9a) \rightarrow (NHC)[PhNi(μ_2 -I)] ₂ (NHC) (14) + 2THF	-20.2	-26.8
2(THF)[PhNiI](NHC) (9b) \rightarrow (NHC)[PhNi(μ_2 -I)] ₂ (NHC) (14) + 2THF	1.0	-8.7
2(THF)[PhNiI](NHC) (9c) \rightarrow (NHC)[PhNi(μ_2 -I)] ₂ (NHC) (14) + 2THF	-7.2	-14.8
<i>M = Pd</i>		
2(THF)[PhPdI](NHC) (9a) \rightarrow (NHC)[PhPd(μ_2 -I)] ₂ (NHC) (14) + 2THF	-28.5	-35.1
2(THF)[PhPdI](NHC) (9b) \rightarrow (NHC)[PhPd(μ_2 -I)] ₂ (NHC) (14) + 2THF	-2.2	-11.0
2(THF)[PhPdI](NHC) (9c) \rightarrow (NHC)[PhPd(μ_2 -I)] ₂ (NHC) (14) + 2THF	-6.2	-14.7

Table S52. Computed (free) energies of the competing **2a** \rightarrow **6a** and **2a** \rightarrow **5a** transformations (and **9a** \rightarrow **12a** vs. **9a** \rightarrow **11a**) in THF.

Formed intermediate	ΔE_r	ΔG_r	ΔE_r	ΔG_r	Formed intermediate
2a \rightarrow 6a or 9a \rightarrow 12a			2a \rightarrow 5a or 9a \rightarrow 11a		
<i>M = Ni</i>			<i>M = Ni</i>		
12a ; L ₁ = NHC; L ₂ = THF	-6.4	-3.0	-3.5	-1.2	11a ; L ₁ = NHC; L ₂ = THF
12a ; L ₁ = L ₂ = NHC	-7.2	-3.9	-6.2	-3.3	11a ; L ₁ = L ₂ = NHC
6a ; L = PMe ₃	-6.8	-2.5	-4.5	-0.6	5a ; L = PMe ₃
6a ; L = PPh ₃	-6.3	-3.2	-2.9	1.7	5a ; L = PPh ₃
<i>M = Pd</i>			<i>M = Pd</i>		
12a ; L ₁ = NHC; L ₂ = THF	-7.5	-3.7	-4.4	-1.0	11a ; L ₁ = NHC; L ₂ = THF
12a ; L ₁ = L ₂ = NHC	-6.9	-3.8	-5.7	-2.4	11a ; L ₁ = L ₂ = NHC
6a ; L = PMe ₃	-9.4	-5.5	-5.1	-1.8	5a ; L = PMe ₃
6a ; L = PPh ₃	-14.9	-9.8	-10.2	-5.9	5a ; L = PPh ₃

Table S53. Computed (free) energies of the **7** (**13**) formation from the intermediates **2a** and **6a** (**9a** and **12a**) in THF.

Formed intermediate	ΔE_r	ΔG_r^a	ΔG_r^b	ΔE_r	ΔG_r^a	ΔG_r^b
	6a \rightarrow 7 or 12a \rightarrow 13			2a \rightarrow 7 or 9a \rightarrow 13		
	<i>M = Ni</i>			<i>M = Ni</i>		
13 ; L ₁ = NHC; L ₂ = THF	12.7	1.5	0.0	6.3	-1.5	-4.5
13 ; L ₁ = L ₂ = NHC	12.1	0.9	-0.6	4.8	-3.0	-6.0
7 ; L = PMe ₃	12.7	1.9	0.4	5.9	-0.6	-3.6
7 ; L = PPh ₃	12.4	2.2	0.7	6.2	-1.0	-4.0
	<i>M = Pd</i>			<i>M = Pd</i>		
13 ; L ₁ = NHC; L ₂ = THF	13.3	2.1	0.6	5.7	-1.6	-4.6
13 ; L ₁ = L ₂ = NHC	11.4	0.5	-1.0	4.4	-3.3	-6.3
7 ; L = PMe ₃	13.9	2.5	1.1	4.5	-3.0	-5.9
7 ; L = PPh ₃	13.8	1.1	-0.3	-1.1	-8.6	-11.6

^a with the THF concentration correction term added (Equation (2) in the Computational Details section of the main text); ^b no THF concentration correction applied (the Gibbs free energy of an isolated THF molecule was calculated via Equation (1) in the Computational Details section of the main text).

Table S54. Computed (free) energies of the competing **2b** \rightarrow **6b** and **2b** \rightarrow **5b** transformations (and **9b** \rightarrow **12b** vs. **9b** \rightarrow **11b**) in THF.

Formed intermediate	ΔE_r	ΔG_r	ΔE_r	ΔG_r	Formed intermediate
2b \rightarrow 6b or 9b \rightarrow 12b			2b \rightarrow 5b or 9b \rightarrow 11b		
	<i>M = Ni</i>		<i>M = Ni</i>		
12b ; L ₁ = NHC; L ₂ = THF	-10.9	-7.8	-5.8	-3.1	11b ; L ₁ = NHC; L ₂ = THF
12b ; L ₁ = L ₂ = NHC	-2.9	1.7	-0.6	3.8	11b ; L ₁ = L ₂ = NHC
6b ; L = PMe ₃	-6.3	-3.0	-4.8	-2.0	5b ; L = PMe ₃
6b ; L = PPh ₃	-12.4	-8.5	-9.1	-5.7	5b ; L = PPh ₃
	<i>M = Pd</i>		<i>M = Pd</i>		
12b ; L ₁ = NHC; L ₂ = THF	-6.0	-2.1	-3.0	0.3	11b ; L ₁ = NHC; L ₂ = THF
12b ; L ₁ = L ₂ = NHC	-9.5	-5.7	-7.1	-3.4	11b ; L ₁ = L ₂ = NHC
6b ; L = PMe ₃	-7.8	-5.2	-6.4	-2.9	5b ; L = PMe ₃
6b ; L = PPh ₃	-13.5	-9.2	-8.9	-4.5	5b ; L = PPh ₃

3. QTAIM Analysis Results

Table S55. Computed QTAIM parameters of the M-Zn-bonding interaction (M = Ni, Pd) in **4a-c**.

Ligand	Intermediate	ρ_b	$\nabla^2\rho_b$	$\frac{G(r_b)}{\rho_b}$	$\frac{h_e(r_b)}{\rho_b}$	$\delta(M,Zn)$	ε_b	$q(M)^a$	$q(Zn)^a$
L = PPh₃	4a ; M = Ni; X = Cl ^b	0.0464	0.0743	0.6358	-0.2349	0.4546	0.1051	0.0945 (0.1296)	1.1003 (-0.0952)
	4a ; M = Pd; X = Cl ^b	0.0376	0.0721	0.6516	-0.1729	0.3277	0.1357	-0.1377 (0.0924)	1.1539 (-0.0416)
	4a ; M = Ni; X = Br ^b	0.0479	0.0740	0.6242	-0.2380	0.4944	0.0617	0.0662 (0.1013)	1.0158 (-0.0916)
	4a ; M = Pd; X = Br ^b	0.0397	0.0762	0.6524	-0.1738	0.3644	0.1176	-0.1525 (0.0776)	1.0702 (-0.0372)
	4a ; M = Ni; X = I ^b	0.0482	0.0715	0.6100	-0.2386	0.5258	0.0665	0.0203 (0.0554)	0.8972 (-0.0652)
	4a ; M = Pd; X = I ^b	0.0425	0.0815	0.6588	-0.1788	0.4170	0.0846	-0.1888 (0.0413)	0.9508 (-0.0116)
L = PMe₃	4c ; M = Ni; X = Cl ^b	0.0589	0.0704	0.5620	-0.2632	0.6435	0.0559	0.1137 (0.2192)	0.8991 (-0.2964)
	4b ; M = Pd; X = Cl	0.0501	0.1119	0.7345	-0.1756	0.5633	0.0135	-0.2328 (0.039)	1.0208 (-0.1747)
	4c ; M = Ni; X = Br ^b	0.0580	0.0711	0.5672	-0.2603	0.6462	0.0510	0.0730 (0.1785)	0.8514 (-0.2560)
	4b ; M = Pd; X = Br	0.0508	0.1148	0.7402	-0.1752	0.5703	0.0135	-0.2275 (0.0443)	0.9330 (-0.1744)
	4c ; M = Ni; X = I ^b	0.0574	0.0775	0.5923	-0.2561	0.6488	0.0271	0.0132 (0.1187)	0.7901 (-0.1723)
	4a ; M = Pd; X = I	0.0478	0.1026	0.7134	-0.1778	0.4788	0.0292	-0.2220 (0.0498)	0.9288 (-0.0336)

ρ_b is the electron density in the BCP, $\nabla^2\rho_b$ is the electron density Laplacian in the BCP, ε_b is the bond ellipticity, $G(r_b)$ is the positive definite kinetic energy density in the BCP, $h_e(r_b)$ is the electron energy density in the BCP, $\delta(M,Zn)$ is the QTAIM delocalization index of M-Zn bond, $q(M)$ and $q(Zn)$ are Ni (Pd) and Zn Bader charges, respectively. ^a $\Delta q(A)$ values (the Bader charge increase or decrease upon the formation of the intermetallic species) are in parentheses. ^b Automatic choice of the integration algorithm (AIMAll default, see the Computational Details section of the main text).

4. Relaxed Surface Scan Results

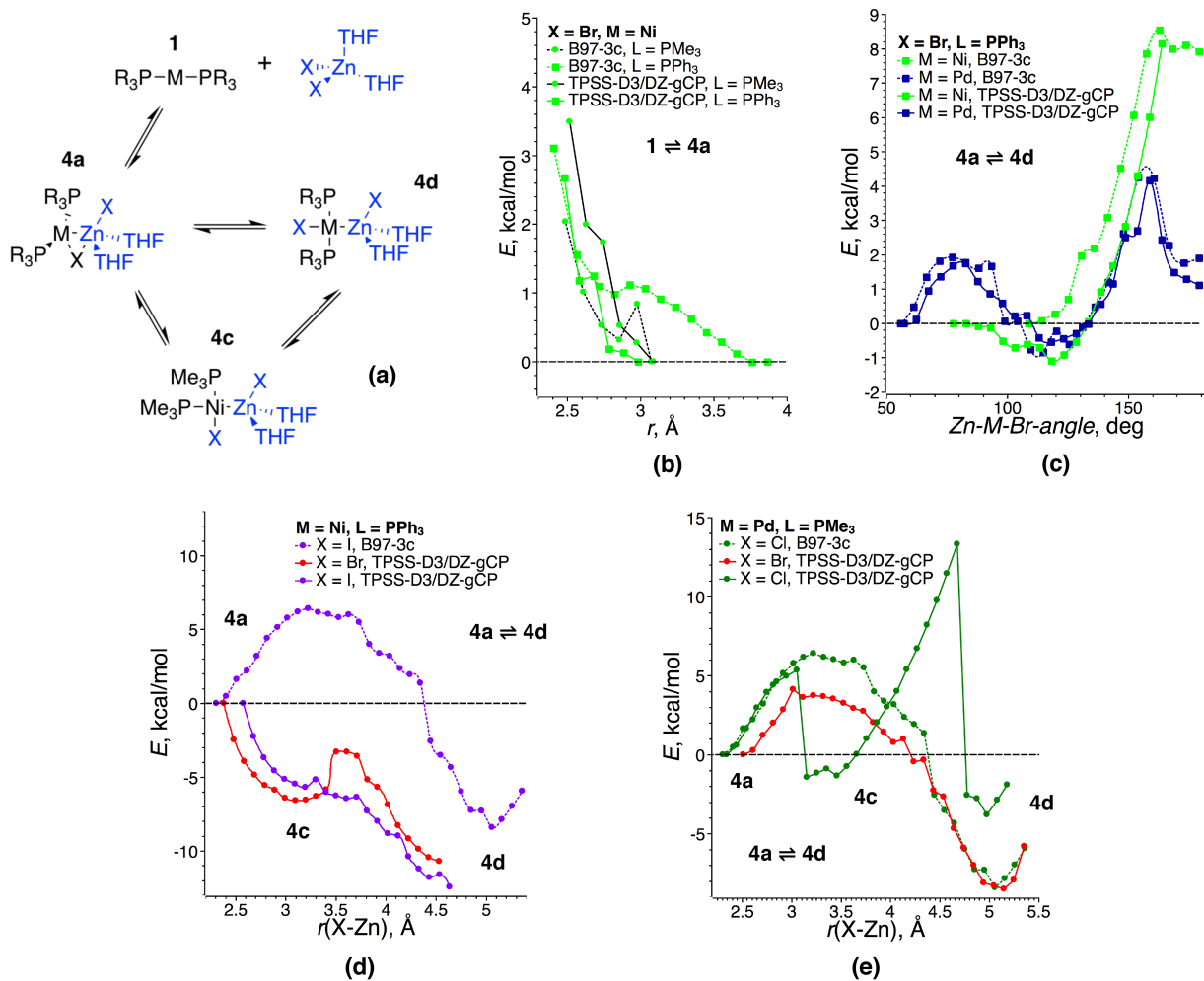


Figure S1. Schematic representation of the 4a formation and 4a-c interconversions – (a); the corresponding relaxed PES scans – (b)-(e). Connecting lines are given only to guide the eye.

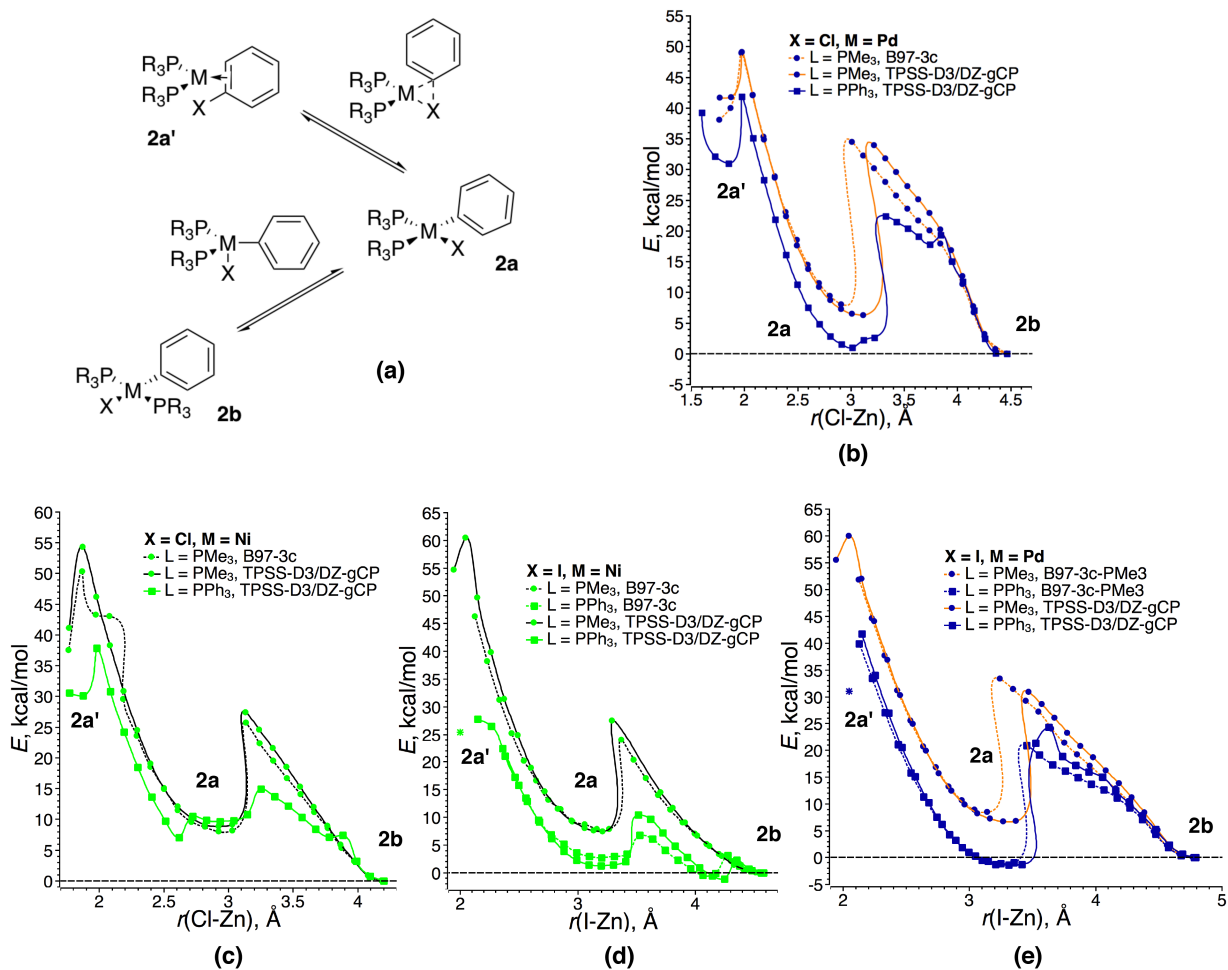


Figure S2. Schematic representations of the modeled oxidative addition and $\text{PR}_3[\text{PhMX}]\text{PR}_3$ cis-trans isomerization processes – (a); the corresponding relaxed potential energy surface scans – (b)–(e). As long as no transition state optimization procedures were done, the structures above the double-sided arrows in (a) are given for convenience only (they represent structures of the complexes in local maxima of the plotted relaxed PES scans). Connecting lines are given only to guide the eye.

5. Total and relative energies of Li zincate species

The relative energies of zincate species were computed according to the following equations:

$$\Delta E_{rel}^{Li[(THF)EtZnBr_2]} = E^{Li[(THF)EtZnBr_2]} + E^{[(THF)_2PhZnBr]} + E^{[(THF)_2ZnBr_2]} \\ - (E^{[(THF)_2EtZnBr]} + E^{[(THF)_2PhZnBr]} + E^{Li[(THF)ZnBr_3]})$$

$$\Delta E_{rel}^{Li[(THF)PhZnBr_2]} = E^{[(THF)_2EtZnBr]} + E^{Li[(THF)PhZnBr_2]} + E^{[(THF)_2ZnBr_2]} \\ - (E^{[(THF)_2EtZnBr]} + E^{[(THF)_2PhZnBr]} + E^{Li[(THF)ZnBr_3]})$$

$$\Delta E_{rel}^{Li_2[EtZnBr_3]} = E^{Li_2[EtZnBr_3]} + E^{[(THF)_2PhZnBr]} + E^{[(THF)_2ZnBr_2]} \\ - (E^{[(THF)_2EtZnBr]} + E^{[(THF)_2PhZnBr]} + E^{Li_2[ZnBr_4]})$$

$$\Delta E_{rel}^{Li_2[PhZnBr_3]} = E^{[(THF)_2EtZnBr]} + E^{Li_2[PhZnBr_3]} + E^{[(THF)_2ZnBr_2]} \\ - (E^{[(THF)_2EtZnBr]} + E^{[(THF)_2PhZnBr]} + E^{Li_2[ZnBr_4]})$$

Table 56. Absolute energies of Li zincates, RZnBr, and ZnBr₂ in THF (C-PCM model), in Hartree.

$E^{[(THF)_2EtZnBr]} = -4896.90832165$	$E^{[(THF)_2PhZnBr]} = -5049.28088710$	$E^{[(THF)_2ZnBr_2]} = -7391.56168413$
$E^{Li[(THF)EtZnBr_2]} = -7245.97606850$	$E^{Li[(THF)PhZnBr_2]} = -7398.34772606$	$E^{Li[(THF)ZnBr_3]} = -9740.63053691$
$E^{Li_2[EtZnBr_3]} = -9595.03768936$	$E^{Li_2[PhZnBr_3]} = -9747.40262668$	$E^{Li_2[ZnBr_4]} = -12089.69588175$

The values were computed according to Equation (1) of this SI file at the RI-TPSS-D3(BJ)/ma-def2-SVP level.

6. Thermodynamics of the formation of Zn-M(II)-intermetallic species in NHC-ligand catalytic systems

We considered the conventional M(0)/M(II) cycle in Ni and Pd catalytic systems with mono- and bis-NHC-ligand species (Figure 6 of the main text). In the mono-ligand systems, THF molecules were added to the metal coordination sphere to obtain coordinatively-saturated model species (L = THF in Figure 9). With Ni-NHC catalysts, the sequence of the elementary steps in the catalytic cycle may diverge from the conventional one because of potential involvement of radical pathways (making, for example, the Ni(I)/Ni(III) cycle operational).³³ The Ni(0)/Ni(II) and Ni(I)/Ni(III) cycles are known to be interconnected under catalytic conditions via comproportionation.³⁴⁻³⁶ It should also be noted that product inhibition in Pd-NHC catalytic systems was demonstrated (in the absence of a LiX salt additive).³⁷⁻⁴⁰

As in the aforementioned phosphine systems, the pre-transmetalation NHC complexes **11a(b)** may form along with the off-cycle intermetallic species **12a(b)** and **13**. The relative stability of the in- and off-cycle species may be rationalized through examining $\Delta\Delta G_{4-6}$ values (see Table S57; negative values indicate that the **12a(b)** and **13** formation is more favorable).

The same discrepancy between the B97-3c and TPSS-D3/DZP results was observed in NHC systems. The formation free energies of the intermediates **11a**, **12a**, **11b**, and **12b** increased in the row Cl < Br < I, according to the TPSS-D3/DZP calculations (see the SI Section 2). For X = Cl, all **9a**→**11a**, **9a**→**12a**, **9b**→**11b**, and **9b**→**12b** processes were exergonic while, for X = I, all transformations were endergonic. In the case of X = Br, **9a**→**12a** and **9b**→**12b** were exergonic, as well as endergonic, depending on the metal and the number of ligands; all **9a**→**11a** and **9b**→**11b** transformations were endergonic. Similarly, to the aforementioned case of L = PR₃, no such trends in the relative reaction free energies of the processes **2a**→**5a**, **2a**→**6a**, **2b**→**5b**, and **2b**→**6b** with

the variation of X were observed in the B97-3c results. The off-cycle species **13** were unstable in THF solutions (i.e., the **9a**→**13** reaction was endergonic), according to the modeling at the B97-3c level. **13** formation was exergonic in THF for M = Pd, X = Br and I at the TPSS-D3/DZP level.

Table S57. Computed $\Delta\Delta G$ values (competitive formation of **12a(b)** and **13** vs. **11a(b)** in THF).

	$\Delta\Delta G_4$: 9a → 12a vs. 9a → 11a		$\Delta\Delta G_5$: 9a → 13 vs. 9a → 11a		$\Delta\Delta G_6$: 9b → 12b vs. 9b → 11b	
	M = Ni	M = Pd	M = Ni	M = Pd	M = Ni	M = Pd
X = Cl						
L = THF	-0.8 ^a (-2.2) ^b	-2.9 (-2.6)	0.4 (0.5)	-2.0 (-2.0)	-3.0 (-2.3)	-3.3 (-3.9)
L = <i>i</i> -Pr-Im	-1.2 (-1.4)	-1.6 (-1.8)	-0.6 (4.5)	-1.6 (0.0)	-3.7 (-3.0)	-2.2 (-3.4)
X = Br						
L = THF	-1.8 (-1.0)	-3.7 (-2.0)	-0.7 (-2.7)	-1.3 (-3.5)	-1.3 (-4.7)	-3.2 (-1.5)
L = <i>i</i> -Pr-Im	-2.1 (-1.5)	-1.7 (-1.3)	-1.5 (0.0)	-4.7 (-3.8)	-3.4 (-3.3)	-3.1 (-2.7)
X = I						
L = THF	-1.8 (1.2)	-2.7 (0.7)	-0.3 (-0.2)	-0.6 (-0.4)	-4.8 (0.1)	-2.4 (2.9)
L = <i>i</i> -Pr-Im	-0.6 (1.2)	-1.4 (1.2)	0.3 (3.7)	-0.9 (-0.6)	-2.1 (0.7)	-2.3 (0.7)

^a Without parentheses: computed at the B97-3c level; ^b in parentheses: computed at the TPSS-D3/DZP level. Negative values indicate that the **12a(b)** and **13** formation is more exergonic than the formation of **11a(b)**.

7. References

- 1 F. Neese, *Wiley Interdiscip. Rev. Comput. Mol. Sci.*, 2012, **2**, 73.
- 2 J. G. Brandenburg, C. Bannwarth, A. Hansen and S. Grimme, *J. Chem. Phys.*, 2018, **148**, 064104.
- 3 A. D. Becke, *J. Chem. Phys.*, 1998, **107**, 8554.
- 4 E. J. Baerends, D. E. Ellis and P. Ros, *Chem. Phys.*, 1973, **2**, 41.
- 5 B. I. Dunlap, J. W. D. Connolly and J. R. Sabin, *J. Chem. Phys.*, 1979, **71**, 3396.
- 6 C. Van Alsenoy, *J. Comput. Chem.*, 1988, **9**, 620.
- 7 R. A. Kendall and H. A. Früchtl, *Theor. Chim. Acta*, 1997, **97**, 158.
- 8 K. Eichkorn, F. Weigend, O. Treutler and R. Ahlrichs, *Theor. Chim. Acta*, 1997, **97**, 119.
- 9 K. Eichkorn, O. Treutler, H. Öhm, M. Häser and R. Ahlrichs, *Chem. Phys. Lett.*, 1995, **240**, 283.
- 10 J. L. Whitten, *J. Chem. Phys.*, 1973, **58**, 4496.
- 11 J. Tao, J. P. Perdew, V. N. Staroverov and G. E. Scuseria, *Phys. Rev. Lett.*, 2003, **91**, 146401.
- 12 S. Grimme, J. Antony, S. Ehrlich and H. Krieg, *J. Chem. Phys.*, 2010, **132**, 154104.
- 13 S. Grimme, S. Ehrlich and L. Goerigk, *J. Comput. Chem.*, 2011, **32**, 1456.
- 14 H. Kruse and S. Grimme, *J. Chem. Phys.*, 2012, **136**, 154101.
- 15 F. Weigend and R. Ahlrichs, *Phys. Chem. Chem. Phys.*, 2005, **7**, 3297.
- 16 D. Andrae, U. Häußermann, M. Dolg, H. Stoll and H. Preuß, *Theor. Chim. Acta*, 1990, **77**, 123.
- 17 K. A. Peterson, *J. Chem. Phys.*, 2003, **119**, 11099.
- 18 F. Weigend, *Phys. Chem. Chem. Phys.*, 2006, **8**, 1057.
- 19 S. Grimme, *Chem. - A Eur. J.*, 2012, **18**, 9955.

- 20 V. Barone and M. Cossi, *J. Phys. Chem. A*, 1998, **102**, 1995.
- 21 E. van Lenthe, E. J. Baerends and J. G. Snijders, *J. Chem. Phys.*, 1993, **99**, 4597.
- 22 C. van Wüllen, *J. Chem. Phys.*, 1998, **109**, 392.
- 23 D. A. Pantazis, X.-Y. Chen, C. R. Landis and F. Neese, *J. Chem. Theory Comput.*, 2008, **4**, 908.
- 24 AIMAll (Version 17.01.25), Todd A. Keith, TK Gristmill Software, Overland Park KS, USA, 2017 (aim.tkgristmill.com)
- 25 F. W. Biegler-König, R. F. W. Bader and T.-H. Tang, *J. Comput. Chem.*, 1982, **3**, 317.
- 26 J. Zheng, X. Xu and D. G. Truhlar, *Theor. Chem. Acc.*, 2011, **128**, 295.
- 27 J. Ho, A. Klamt and M. L. Coote, *J. Phys. Chem. A*, 2010, **114**, 13442.
- 28 A. Hellweg and F. Eckert, *AIChE J.*, 2017, **63**, 3944.
- 29 R. F. Ribeiro, A. V. Marenich, C. J. Cramer and D. G. Truhlar, *J. Phys. Chem. B*, 2011, **115**, 14556.
- 30 ORCA Common Errors and Problems - ORCA Input Library, <https://sites.google.com/site/orcainputlibrary/orca-common-problems>, (accessed 17 June 2019).
- 31 E. F. Valeev, Libint is a High-performance Library for Computing Gaussian Integrals in Quantum Mechanics, <https://github.com/evaleev/libint>, (accessed 12 October 2018).
- 32 U. Ekström, L. Visscher, R. Bast, A. J. Thorvaldsen and K. Ruud, *J. Chem. Theory Comput.*, 2010, **6**, 1971.
- 33 M. Henrion, V. Ritleng and M. J. Chetcuti, *ACS Catal.*, 2015, **5**, 1283.
- 34 M. Mohadjer Beromi, A. Nova, D. Balcells, A. M. Brasacchio, G. W. Brudvig, L. M. Guard, N. Hazari and D. J. Vinyard, *J. Am. Chem. Soc.*, 2017, **139**, 922.

- 35 S. Bajo, G. Laidlaw, A. R. Kennedy, S. Sproules and D. J. Nelson, *Organometallics*, 2017, **36**, 1662.
- 36 D. D. Beattie, G. Lascoumettes, P. Kennepohl, J. A. Love and L. L. Schafer, *Organometallics*, 2018, **37**, 1392.
- 37 R. Jana, T. P. Pathak and M. S. Sigman, *Chem. Rev.*, 2011, **111**, 1417.
- 38 H. N. Hunter, N. Hadei, V. Blagojevic, P. Patschinski, G. T. Achonduh, S. Avola, D. K. Bohme and M. G. Organ, *Chem. - A Eur. J.*, 2011, **17**, 7845.
- 39 L. C. McCann, H. N. Hunter, J. A. C. Clyburne and M. G. Organ, *Angew. Chem. Int. Ed.*, 2012, **51**, 7024.
- 40 L. C. McCann and M. G. Organ, *Angew. Chem. Int. Ed.*, 2014, **53**, 4386.